AAS 07-267

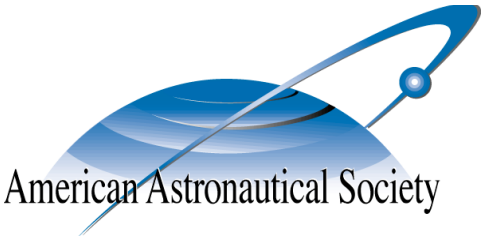

American Institute of
Aeronautics and Astronautics

1-D CONSTRAINED COULOMB STRUCTURE STABILIZATION WITH CHARGE SATURATION

Shuquan Wang and Hanspeter Schaub

Astrodynamics Specialist Conference

Mackinac Island, Michigan August 19–23, 2007

AAS Publications Office, P.O. Box 28130, San Diego, CA 92198

AAS 07-267

1-D CONSTRAINED COULOMB STRUCTURE STABILIZATION WITH CHARGE SATURATION

Shuquan Wang* **and Hanspeter Schaub†**

A Coulomb structure is a cluster of free-flying satellites which maintains its shape through inter-vehicle electrostatic forces. These Coulomb forces are generated using on-board charge emission devices. This paper investigates the 1-D restricted motion of a 3-craft cluster. Two charge feedback strategies are discussed where the charge saturation limitation is considered. First a unsaturated formation shape feedback control strategy is presented. Next, a saturated control strategy is developed to arrest any relative motion rates of the Coulomb structure. If the structure can be brought to rest, then the unsaturated charge control is engaged to achieve the desired virtual structure. The saturated feedback control development is developed using Lyapunov's direct method and can control the separation rates between the satellites by changing the signs of the three saturated charge products. Implementable real-charge solutions are ensured through scaling the Lyapunov function rate. The control is shown to be Lyapunov stable. Because of the limitation of the control charge magnitudes, certain initial conditions will not lead to the desired zero relative motion rates. Conditions under which the relative motion of the Coulomb structure can be stabilized are analyzed through investigating the total energy of the system in the symmetric motion assumption. The general converge areas are illustrated numerically in the phase planes. Simulations demonstrate the performance of the control.

1 INTRODUCTION

King et al.[1] originally discussed the novel method of exploiting Coulomb forces for formation flying in 2002. Since then many papers have been published in this area. Coulomb forces are proposed to control a tight formation with separation distances up to 100 meters. Electrostatic force fields are generated to control the formation's shape and size. There are some other promising techniques in close formation flying such as the Electric Propulsion(EP)[1] and Electro-Magnetic Formation Flying(EMFF).[2] EP systems generate forces by expelling ionic plumes. The ionic plumes can disturb the motions of nearby spacecraft, and the intensive and caustic charge plumes are also threatening to sensitive instruments. The EMFF method controls relative separation and attitude of the formation by creating electromagnetic dipoles on each spacecraft in concert with reaction wheels. In contrast to the EP method, the Coulomb formation flying technique has no exhausting plume contamination issues. The Coulomb force field is also simpler to model than the electromagnetic force field, and the strength does not drop off as fast as electromagnetic force field. The generation of Coulomb forces has been shown to require only Watt-level of power, and can be controlled on a millisecond time scale.[3] In addition, Coulomb force control is 3-5 orders of magnitude more fuel-efficient than EP.[1] This is an essential advantage in long-term space missions.

*Graduate Research Assistant, Aerospace Engineering Science Department, Colorado University, CO,
†Associate Professor, Aerospace Engineering Science Department, Colorado University, CO.

Many challenges in Coulomb formation flying have been investigated. Hyunsik Joe et al. introduced a formation coordinate frame which tracked the principal axes of the formation in Reference 4. Gordon G. Parker et al. presented a sequential control strategy for arranging N charged bodies into an arbitrary geometry using $N + 3$ participating bodies in Reference 5. This paper overcame two challenging problems of Coulomb force control: the Coulomb force coupling and unimplementable control solutions arising from the quadratic charge nonlinearity. First order differential orbit element constraints for Coulomb formation are studied in Reference 6. Arun Natarajan et al. developed charge feedback laws to stabilize the relative distance between two satellites of a Coulomb tether formation in References 7, 8 and 9. For the nadir-aligned 2 craft case the in-plane attitude of the Coulomb tether formation can also be stabilized by exploiting the gravity gradient torque.

This paper discusses the control of a 1-D restricted 3-craft Coulomb virtual structure. A Coulomb structure is a virtual structure composed of several spacecraft. The structure's shape and size is controlled by utilizing the inter-spacecraft electrostatic forces. This virtual structure control can be used in large scale distributed spacecraft concepts. The general three-dimensional charged spacecraft motion is very complex, and its control is an open area of research. This paper focuses on the 1-D restricted 3-craft Coulomb virtual structure to investigate charge implementability issues and charge saturation limitations. This control is directly applicable to the control of three charged test vehicles on a non-conducting hover track. Such a test bed is envisioned to perform basic charged vehicle relative motion control experiments.

Reference 10 designs a charge feedback strategy which stabilizes the shape and size of a 1-D restricted Coulomb structure to a desired configuration. Reference 10 also presents a method to exploit the nullspace to determine implementable (i.e. non-imaginary) charge solutions. This paper will present a modified version of this control which uses the relative kinematic energy as the Lyapunov function. This leads to a simpler control solution. The craft are assumed to only experience electrostatic forces. No orbital motion is modeled. Instead, the equations of motion are applicable for a 1-D charged vehicle test track. The relative kinetic energy is then used to provide bounds on the initial conditions to guarantee convergence in the presence of charge saturation.

Because of the limited amount of charge that a spacecraft can safely store, the Coulomb structure shape may be not controllable in some situations. For example, if the three spacecraft are departing each other at very high speeds, then the limited actuation capability of the saturated Coulomb forces may not be able to pull them back to construct a virtual structure. This paper designs a saturated control based on Lyapunov's direct method. The control is intended to stabilize the relative rates of the Coulomb structure and stop an initial expansion. Once the motion is stabilized, other control approaches can be used to shape the structure to certain configurations. The magnitudes of the control charges are always kept at their maximum values, the only items that are varying are the signs of these control charges. The control stability is analytically determined, and the regions of convergence investigated.

After the relative motion is stabilized, the unsaturated feedback law for formation shape control is employed to shape the structure to a certain desired configuration. This step completes the two-stage control strategy to control the shape of the 1-D constrained Coulomb structure with charge saturation limits. Numerical simulation will be used to illustrate the effectiveness of the control strategy.

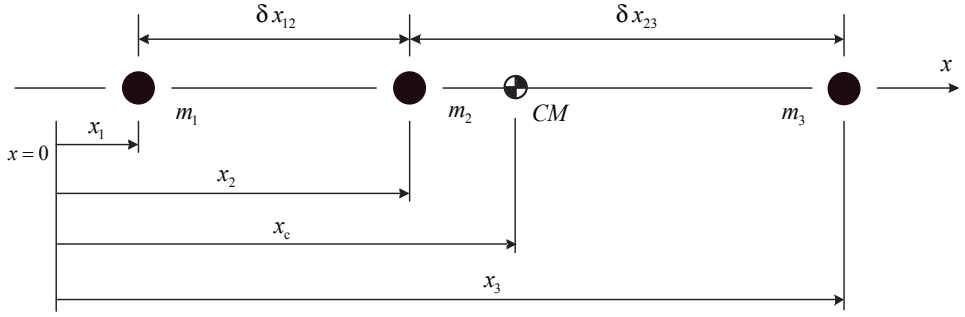

Figure 1 Illustration of 1-D constrained coordinates of the 3-body system.

2 CHARGED EQUATIONS OF MOTION

Let the Coulomb structure consist of 3 bodies with masses m_i, which they are restricted to move in one-dimension only as illustrated in Figure 1. This setup simulates the motion of test vehicles floating on a non-conducting hover track. The inertial positions of the three bodies are given through their inertial coordinates x_i. The charges q_i always appear in pairs $q_i q_j$ both in the dynamic functions and in the control formulation. Charge products are introduced as

$$Q_{ij} = q_i q_j \tag{1}$$

This approach quickly leads to the problem of physical feasibility in extracting individual charges q_i from a given set of charge products. This issue is addressed in the later sections. Without loss of generality, assume that $x_1 < x_2 < x_3$. Let the spacecraft fly freely in space, the inertial equations of motion of the charged bodies are given through

$$m_1 \ddot{x}_1 = k_c \left[-\frac{Q_{12}}{(x_2 - x_1)^2} - \frac{Q_{13}}{(x_3 - x_1)^2} \right] \tag{2}$$

$$m_2 \ddot{x}_2 = k_c \left[\frac{Q_{12}}{(x_2 - x_1)^2} - \frac{Q_{23}}{(x_3 - x_2)^2} \right] \tag{3}$$

$$m_3 \ddot{x}_3 = k_c \left[\frac{Q_{13}}{(x_3 - x_1)^2} + \frac{Q_{23}}{(x_3 - x_2)^2} \right] \tag{4}$$

where $k_c = 8.99 \times 10^9 \mathrm{C}^{-2} \cdot \mathrm{N} \cdot \mathrm{m}^2$ is the Boltzmann's constant. A charge feedback law is required to control the relative motion of the three-body Coulomb structure and make the formation assume a specific shape.

Not all of the inertial x_i states can be controlled independently. Because the spacecraft charges produce formation internal forces, the momentum of the Coulomb cluster must be conserved if there are no other external forces acting on it. As a result it is not possible to directly control all the three inertial coordinates x_i. For the 1D motion considered in this paper, the linear momentum conservation imposes one constraint on the system. Thus, the motion of the three-body system only has two controlled degrees of freedom. To control the shape of the 1D-restricted 3-craft Coulomb structure, it is equivalent to control the two relative distances:

$$\delta x_{12} = x_2 - x_1, \qquad \delta x_{23} = x_3 - x_2 \tag{5}$$

Here the third distance δx_{13} is determined as $\delta x_{13} = \delta x_{12} + \delta x_{23}$. To control the shape of the Coulomb structure is to drive $[\delta x_{12}, \delta x_{23}]^T$ to the desired values $[\delta x_{12}^*, \delta x_{23}^*]^T$ that yield a specific virtual structure shape. Note that the two relative position coordinates are independent coordinates. The momentum conservation has already been incorporated into the relative motion coordinate choice. None of the control strategies presented in this paper will attempt to control the formation cluster's center of mass motion.

From the inertial equations of motion in Eqs. (2)–(4), using the definition of δx_{ij}, the separation distance equations of motion are found to be

$$\delta\ddot{x}_{12} = \ddot{x}_2 - \ddot{x}_1 = k_c \left(\frac{1}{m_1} + \frac{1}{m_2}\right) \frac{Q_{12}}{\delta x_{12}^2} - \frac{k_c}{m_2}\frac{Q_{23}}{\delta x_{23}^2} + \frac{k_c}{m_1}\frac{Q_{13}}{\delta x_{13}^2} \tag{6}$$

$$\delta\ddot{x}_{23} = \ddot{x}_3 - \ddot{x}_2 = -\frac{k_c}{m_2}\frac{Q_{12}}{\delta x_{12}^2} + k_c \left(\frac{1}{m_2} + \frac{1}{m_3}\right) \frac{Q_{23}}{\delta x_{23}^2} + \frac{k_c}{m_3}\frac{Q_{13}}{\delta x_{13}^2} \tag{7}$$

The formation kinetic energy T is a convenient measure to construct a Lyapunov function of the system and analyze the nonlinear stability.

$$T = \frac{1}{2}\sum_{i=1}^{3} m_i \dot{x}_i^2 \tag{8}$$

However, the control goal is not to control the total energy of the system, but rather to control the relative energy which affects the virtual structure shape. Thus the inertial kinetic energy expression in Eq. (8) needs to be rewritten in terms of the relative coordinate rates $\delta\dot{x}_{12}$ and $\delta\dot{x}_{23}$. Taking derivative of Eq. (5) yields

$$\dot{x}_1 = \dot{x}_2 - \delta\dot{x}_{12}, \qquad \dot{x}_3 = \dot{x}_2 + \delta\dot{x}_{23} \tag{9}$$

Substituting Eq. (9) into Eq. (8) leads to

$$T = \frac{M}{2}\dot{x}_2^2 + \frac{m_1}{2}\delta\dot{x}_{12}^2 + \frac{m_3}{2}\delta\dot{x}_{23}^2 + \dot{x}_2(m_3\delta\dot{x}_{23} - m_1\delta\dot{x}_{12}) \tag{10}$$

where $M = \sum_{i=1}^{3} m_i$ is the total mass of the three spacecraft cluster. The expression of the total kinetic energy in Eq. (10) still contains an inertial rate variable $\dot{x}_2$ which cannot be controlled independently with Coulomb forces. One more step to express $\dot{x}_2$ in terms of $\delta\dot{x}_{ij}$ is needed.

Note that the Coulomb forces are internal forces in the Coulomb structure, by assuming the spacecraft to be flying freely in deep space, the following center of mass condition must be true:

$$m_1\dot{x}_1 + m_2\dot{x}_2 + m_3\dot{x}_3 = M\dot{x}_c \tag{11}$$

where x_c is the inertial cluster center of mass coordinate. Utilizing Eq. (11), yields the following algebraic derivations:

$$\begin{aligned} M\dot{x}_2 &= M\dot{x}_2 - m_1\dot{x}_1 - m_2\dot{x}_2 - m_3\dot{x}_3 + M\dot{x}_c \\ &= m_1\dot{x}_2 - m_1\dot{x}_1 + m_2\dot{x}_2 - m_2\dot{x}_2 + m_3\dot{x}_2 - m_3\dot{x}_3 + M\dot{x}_c \\ &= m_1\delta\dot{x}_{12} - m_3\delta\dot{x}_{23} + M\dot{x}_c \end{aligned} \tag{12}$$

Thus $\dot{x}_2$ is expressed in terms of δx_{ij} as:

$$\dot{x}_2 = \frac{1}{M}(m_1\delta\dot{x}_{12} - m_3\delta\dot{x}_{23}) + \dot{x}_c \tag{13}$$

Substituting Eq. (13) into Eq. (10), yields

$$\begin{aligned} T =& \frac{(m_1\delta\dot{x}_{12} - m_3\delta\dot{x}_{23})^2}{2M} + \frac{m_1}{2}\delta\dot{x}_{12}^2 + \frac{m_2}{2}\delta\dot{x}_{23}^2 - \frac{1}{M}(m_1\delta\dot{x}_{12} - m_3\delta\dot{x}_{23})^2 \\ &+ \frac{M}{2}\dot{x}_c^2 + \frac{M}{2}\frac{2}{M}\dot{x}_c(m_1\delta\dot{x}_{12} - m_3\delta\dot{x}_{23}) - \dot{x}_c(m_1\delta\dot{x}_{12} - m_3\delta\dot{x}_{23}) \\ =& \frac{m_1}{2}\delta\dot{x}_{12}^2 + \frac{m_2}{2}\delta\dot{x}_{23}^2 - \frac{1}{2M}(m_1\delta\dot{x}_{12} - m_3\delta\dot{x}_{23})^2 + \frac{M}{2}\dot{x}_c^2 \\ =& \frac{m_1m_2}{2M}\delta\dot{x}_{12}^2 + \frac{m_1m_3}{2M}(\delta\dot{x}_{12} + \delta\dot{x}_{23})^2 + \frac{m_2m_3}{2M}\delta\dot{x}_{23}^2 + \frac{M}{2}\dot{x}_c^2 \\ =& \frac{1}{2}\dot{\boldsymbol{X}}^T[M]\dot{\boldsymbol{X}} + \frac{M}{2}\dot{x}_c^2 \end{aligned} \tag{14}$$

where $[M]$ is the system mass matrix:

$$[M] = \frac{1}{M}\begin{bmatrix} m_1m_2 + m_1m_3 & m_1m_3 \\ m_1m_3 & m_1m_3 + m_2m_3 \end{bmatrix} \tag{15}$$

Finally, the kinetic energy T_{rel} of the 3-craft cluster relative to the center of mass is given by

$$T_{\text{rel}} = \frac{1}{2}\dot{\boldsymbol{X}}^T[M]\dot{\boldsymbol{X}} \tag{16}$$

This energy expression directly reflects whether the virtual structure shape is changing its geometry with time.

3 CONTROL STRATEGY

3.1 Shape Coordinate Equations of Motion

This section develops a unsaturated feedback control strategy that controls the 1-D 3-body formation to a certain desired shape. The desired shape is given by a vector of separation distances $[\delta x_{12}^*,\ \delta x_{23}^*]^T$, and it's assumed to be stationary (i.e. constant desired shape).

For the control development, let the system state vector $\boldsymbol{X}$ define to be the relative distance tracking error:

$$\boldsymbol{X} = \begin{bmatrix} \Delta x_{12} \\ \Delta x_{23} \end{bmatrix} = \begin{bmatrix} \delta x_{12} - \delta x_{12}^* \\ \delta x_{23} - \delta x_{23}^* \end{bmatrix} \tag{17}$$

For notational convenience the 3×1 vector $\boldsymbol{\xi}$ is introduced as:

$$\boldsymbol{\xi} = \left[\frac{k_cQ_{12}}{\delta x_{12}^2},\quad \frac{k_cQ_{23}}{\delta x_{23}^2},\quad \frac{k_cQ_{13}}{\delta x_{13}^2}\right]^T = k_c[D]\boldsymbol{Q} \tag{18}$$

where $[D] = \text{diag}\left(\frac{1}{\delta x_{12}^2}, \frac{1}{\delta x_{23}^2}, \frac{1}{\delta x_{13}^2}\right)$ is a diagonal matrix, $\boldsymbol{Q} = [Q_{12}, Q_{23}, Q_{13}]^T$ is a vector of the charge products. The vector $\boldsymbol{Q}$ is also the control input of the Coulomb structure control system. Because the desired relative position coordinates are constants, the tracking error dynamics is

expressed using $\boldsymbol{X}$ as

$$\ddot{\boldsymbol{X}} = \underbrace{\begin{bmatrix} \frac{1}{m_1}+\frac{1}{m_2} & -\frac{1}{m_2} & \frac{1}{m_1} \\ -\frac{1}{m_2} & \frac{1}{m_2}+\frac{1}{m_3} & \frac{1}{m_3} \end{bmatrix}}_{[A]} \boldsymbol{\xi} = k_c[A][D]\boldsymbol{Q} \tag{19}$$

3.2 Formation Shape Control

The controller in this subsection is intended to make the formation attain a certain shape where both $\dot{\boldsymbol{X}}$ and $\boldsymbol{X}$ are driven to zero. The control development does not yet consider spacecraft charge saturation issues.

3.2.1 Minimum Norm Shape Stabilizing Control

Because the state $\boldsymbol{X}$ and the time derivative of the state $\dot{\boldsymbol{X}}$ are all expected to be zero, the Lyapunov function here is defined as a quadratic function of $\boldsymbol{X}$ and $\dot{\boldsymbol{X}}$ as

$$V_1 = \frac{1}{2}\dot{\boldsymbol{X}}^T[M]\dot{\boldsymbol{X}} + \frac{1}{2}\boldsymbol{X}^T[K]\boldsymbol{X} \tag{20}$$

Note that the first term in V_1 is the relative kinetic energy T_{rel} of the system.

Differentiating Eq. (20) with respect to time, and utilizing the shape error EOM in Eq. (19), yields

$$\dot{V}_1 = \dot{\boldsymbol{X}}^T[K]\dot{\boldsymbol{X}} + \dot{\boldsymbol{X}}^T[M]\ddot{\boldsymbol{X}} = \dot{\boldsymbol{X}}^T\Big([K]\boldsymbol{X} + [M][A]\boldsymbol{\xi}\Big) \tag{21}$$

Denote $[C] = [M][A]$, the matrix $[C]$ turns out to be a constant matrix with the following simple form:

$$[C] = \begin{bmatrix} 1 & 0 & 1 \\ 0 & 1 & 1 \end{bmatrix} \tag{22}$$

Next the Lyapunov function rate V_1 is set to the negative semi-definite form

$$\dot{V}_1 = -\dot{\boldsymbol{X}}^T[R]\dot{\boldsymbol{X}} \tag{23}$$

where $[R]$ is a 2×2 positive definite matrix. $\dot{V}_1$ is negative semi-definite because V_1 is a function of both $\dot{\boldsymbol{X}}$ and $\boldsymbol{X}$ but only $\dot{\boldsymbol{X}}$ appears in Eq. (23).

Equating the actual $\dot{V}_1$ in Eq. (21) and the desired $\dot{V}_1$ in Eq. (23) leads to the following feedback control condition:

$$[C]\boldsymbol{\xi} = -[K]\boldsymbol{X} - [R]\dot{\boldsymbol{X}} \tag{24}$$

Solving Eq. (24) for $\boldsymbol{\xi}$ yields the charge products that stabilizes the system. Because $[C]$ only has rank 2, there is an infinite number of solutions for $\boldsymbol{\xi}$ in Eq. (24). Let $\hat{\boldsymbol{\xi}}$ be the minimum norm solution to Eq. (25):

$$\hat{\boldsymbol{\xi}} = -[C]^\dagger\Big([K]\boldsymbol{X} + [R]\dot{\boldsymbol{X}}\Big) \tag{25}$$

Note that $\hat{\boldsymbol{\xi}}$ in Eq. (25) minimizes the norm of the charge products while satisfying Eq. (24), but not the charge inputs q_i of the control. There is a hat symbol above the vector $\boldsymbol{\xi}$ in Eq. (25) because $\hat{\boldsymbol{\xi}}$ is not the final solution of $\boldsymbol{\xi}$ that will be used in the control.

3.2.2 Spacecraft Charge Computation Issues

After obtaining the vector $\boldsymbol{\xi}$, the charge product vector is given by

$$\boldsymbol{Q} = \frac{1}{k_c}[D]^{-1}\boldsymbol{\xi} \tag{26}$$

The individual charges q_i are finally calculated through the algorithm[11]

$$q_1 = \sqrt{\frac{Q_{12}Q_{13}}{Q_{23}}}, \quad q_2 = \text{sign}(Q_{12}) \cdot \frac{Q_{12}}{q_1}, \quad q_3 = \text{sign}(Q_{13}) \cdot \frac{Q_{13}}{q_1} \tag{27}$$

Note that the singularity problem occurs when some elements of $\hat{\boldsymbol{\xi}}$ are equal to zero. When one or two elements of $\hat{\boldsymbol{\xi}}$ equal zero, this singularity can be avoided by performing a search routine in the null space of the $[C]$ matrix which will be discussed in the following several paragraphs. The remaining case is that $\hat{\boldsymbol{\xi}} = \boldsymbol{0}$ which indicates that $q_1 = q_2 = q_3 = 0$. This state occurs only either when $\boldsymbol{X} = 0$ and $\dot{\boldsymbol{X}} = 0$, which means the system has reached the desired state, or due to $(-[K]\boldsymbol{X} - [R]\dot{\boldsymbol{X}})$ being zero.

Now consider general cases where $\hat{\xi}_1 \cdot \hat{\xi}_2 \cdot \hat{\xi}_3 \neq 0$. Note that $\hat{\xi}_1 \cdot \hat{\xi}_2 \cdot \hat{\xi}_3 < 0$ yields imaginary values of q_i.[11] But charges must always be real numbers, so $\hat{\xi}_1 \cdot \hat{\xi}_2 \cdot \hat{\xi}_3 < 0$ is not an implementable solution. This is a fundamental issue with developing any charge feedback law. Note that the $\hat{\boldsymbol{\xi}}$ value is obtained by looking for a minimum norm solutions to the vector $\boldsymbol{\xi}$ in Eq. (24). There is actually an infinite number of solutions that satisfy Eq. (24). Using the null space of $[C]$, all possible $\boldsymbol{\xi}$ values that satisfy Eq. (24) are parameterized as

$$\boldsymbol{\xi} = \begin{pmatrix} \xi_1 \\ \xi_2 \\ \xi_3 \end{pmatrix} = \hat{\boldsymbol{\xi}} + \gamma \begin{pmatrix} -1 \\ -1 \\ 1 \end{pmatrix} \tag{28}$$

where the parameter γ can be any real number. The control problem is reformulated to determine a parameter γ that satisfies the implementability constraint:

$$f(\gamma) = \xi_1 \cdot \xi_2 \cdot \xi_3 = (\hat{\xi}_1 - \gamma)(\hat{\xi}_2 - \gamma)(\hat{\xi}_3 + \gamma) > 0 \tag{29}$$

This inequality constraint guarantees that the charges q_i are real, and also ensures that the singularity case $\xi_1 \cdot \xi_2 \cdot \xi_3 = 0$ does not occur. Because $f(\gamma)$ is a third order function, there always exists real numbers of parameter γ that satisfy the inequality in Eq. (29).

3.2.3 Minimal Charge Search Routine

Any real value of parameter γ that satisfies the inequality in Eq. (29) makes the solution physically implementable with real charge q_i solutions. In fact, note that the null space of the input matrix $[C]$ can be used to charge up the vehicles and not cause any relative motion to occur. The $\hat{\boldsymbol{\xi}}$ vector is found such that the norm of the vector $\boldsymbol{\xi}$ is minimized. However, this doesn't correspond to a more logical optimal solution where the spacecraft charges q_i are minimized. Define a charge cost function $J(\gamma)$ as

$$J(\gamma) = \sum_{i=1}^{3} q_i^2 \tag{30}$$

The optimal solution $\boldsymbol{\xi}$ that minimizes spacecraft charges q_i corresponds to the optimal γ_m that satisfies the inequality constraint in Eq. (29), and at the same time minimizes the charge cost function $J(\gamma)$.

Consider the constraint inequality in Eq. (29), where $(\hat{\xi}_1, \hat{\xi}_2, \hat{\xi}_3)$ are given by Eq. (25). There are three real roots for the equation $f(\gamma) = 0$, and the roots are just $(\hat{\xi}_1, \hat{\xi}_2, -\hat{\xi}_3)$. Rearrange the roots in descent order and denote as $(\gamma_1, \gamma_2, \gamma_3)$, where $\gamma_1 \geq \gamma_2 \geq \gamma_3$. The solution to the constraint in Eq. (29) turns out to be $\gamma > \gamma_1$ or $\gamma_3 < \gamma < \gamma_2$. If $\gamma_2 = \gamma_3$, then the solution is simply $\gamma > \gamma_1$. Figure 2(a) shows a numerical example of $f(\gamma)$ and $(\gamma_1, \gamma_2, \gamma_3)$.

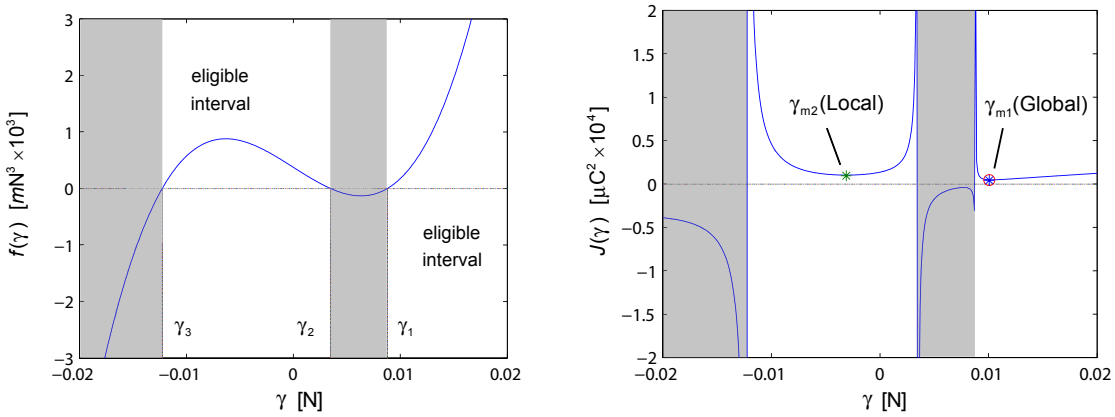

(a) $f(\gamma)$ and $(\gamma_1, \gamma_2, \gamma_3)$. (b) γ_m search result.

Figure 2 Numerical Illustration of Optimal γ_m Search.

Thus the optimization problem searches for the optimal γ_m of the charge cost function $J(\gamma)$ within the two open intervals (γ_1, ∞) and (γ_3, γ_2). The numerical search routine used in this paper is the secant method shown in Figure 3.

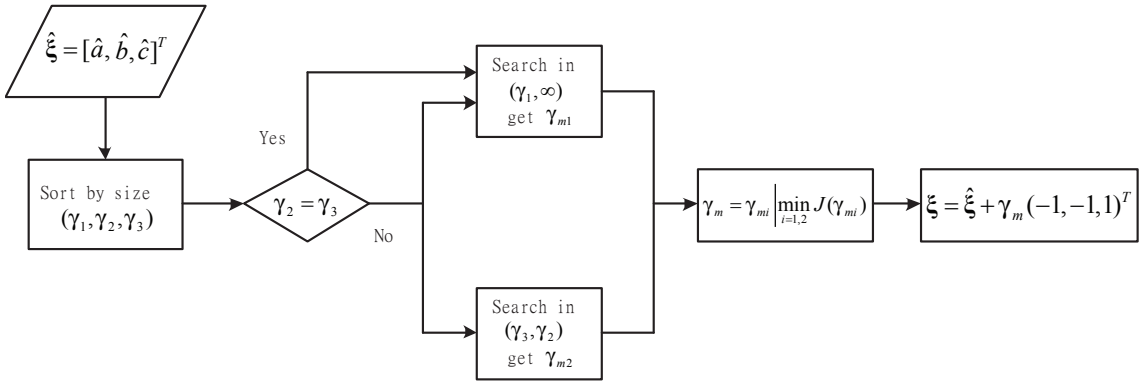

Figure 3 Illustration of γ_m search routine.

Once γ_m is obtained, an implementable solution that minimizes the norm of the charge vector (q_1, q_2, q_3) is also reached. Figure 2 shows an example of the search result at one instant, where γ_{m1} and γ_{m2} are two local optimal points.

Notice that generally there are two eligible intervals in the search routine. Sometimes this may introduce chatter because γ_m switches between γ_{m1} and γ_{m2} when $J(\gamma_{m1})$ and $J(\gamma_{m2})$ are very close. To reduce the chatter of the charge history, one approach is to change the criteria for γ_m to switch between the two intervals. If $\gamma_m(i) = \gamma_{m1}(i)$, then $\gamma_m(i+1) = \gamma_{m2}(i+1)$ if and only if $J(\gamma_{m2}) < \alpha \cdot J(\gamma_{m1})$, where $0 < \alpha \leq 1$.

3.3 Formation Shape Rate Regulation

This subsection develops a regulator that arrests the relative motion of the formation by driving $\dot{\boldsymbol{X}}$ to zero. After developing a saturated stabilizing control strategy a method to obtain implementable spacecraft charges q_i is discussed.

3.3.1 Saturated Regulator

Because the purpose of the control is different from that of the general shape control, thus a new Lyapunov function is defined catering to the new task. Because the regulator is used to stop any relative motion of the formation, the new Lyapunov function V_2 is defined in terms of the relative velocity vector in a quadratic, positive definite form,

$$V_2 = T_{\text{rel}} = \frac{1}{2}\dot{\boldsymbol{X}}^T[M]\dot{\boldsymbol{X}} \tag{31}$$

Taking derivative of V_2, and using the tracking error dynamics in Eq. (19), yields

$$\dot{V}_2 = \dot{\boldsymbol{X}}^T[M]\ddot{\boldsymbol{X}} = k_c\dot{\boldsymbol{X}}^T[C][D]\boldsymbol{Q} \tag{32}$$

The saturated control strategy will attempt to drive the rates $\dot{\boldsymbol{X}}$ to zero as quickly as possible, leading to an Lyapunov optimal control development.[12] Here the spacecraft charges are always held at the maximum magnitude. The control algorithm will need to determine the required signs of the spacecraft charges. The charge product vector $\boldsymbol{Q}$ is expressed as

$$\boldsymbol{Q} = \begin{bmatrix} Q_{12m} & 0 & 0 \\ 0 & Q_{23m} & 0 \\ 0 & 0 & Q_{13m} \end{bmatrix} \begin{bmatrix} s_1 \\ s_2 \\ s_3 \end{bmatrix} = [Q_m]\boldsymbol{s} \tag{33}$$

where $Q_{ijm} = q_{im}q_{jm}$ is the product of the charge saturation limits of the i^{th} and j^{th} spacecraft. The vector $\boldsymbol{s} = \text{sign}(\boldsymbol{Q})$ is a 3×1 sign vector, the components of $\boldsymbol{s}$ can only be ± 1 or zero. The matrix $[Q_m]$ is a constant matrix determined by charge limitations of the spacecraft. Because $[Q_m]$ is constant for a given 3-body Coulomb structure, the charge product $\boldsymbol{Q}$ is determined by $\boldsymbol{s}$, thus the vector $\boldsymbol{s}$ is actually the essential control input which determines the required spacecraft charges. The Lyapunov function rate is rewritten as

$$\dot{V}_2 = k_c\dot{\boldsymbol{X}}^T[C][D][Q_m]\boldsymbol{s} \tag{34}$$

To guarantee stability, the Lyapunov rate function $\dot{V}$ is set to be a negative definite function as

$$\dot{V}_2 = -\dot{\boldsymbol{X}}^T[P]\dot{\boldsymbol{X}} \tag{35}$$

Note that the matrix $[C]$ is a 2×3 matrix with rank 2. Substituting Eq. (35) into Eq. (34), there will be an infinite number of solutions for $\boldsymbol{s}$ if $\boldsymbol{s}$ is a general vector instead of a sign vector. Using the pseudo-inverse of matrix $[C]$, leads to the minimum norm solution $\tilde{\boldsymbol{s}}$ (the tilde symbol means $\tilde{\boldsymbol{s}}$ is not a sign vector that will be directly used in the control) :

$$\tilde{\boldsymbol{s}} = -\frac{1}{k_c}[Q_m]^{-1}[D]^{-1}[C]^{\dagger}[P]\dot{\boldsymbol{X}} \tag{36}$$

where $[C]^{\dagger} = [C]^T([C][C]^T)^{-1}$ is the minimum norm pseudo-inverse of matrix $[C]$. The vector $\tilde{\boldsymbol{s}}$ is said to be nominal because this solution is not a sign vector, that is, the components in $\tilde{\boldsymbol{s}}$ are not restricted to be ± 1 or zero. Define a sign vector $\boldsymbol{s}$ as

$$\boldsymbol{s} = \text{sign}(\tilde{\boldsymbol{s}}) = -\text{sign}\left(\frac{1}{k_c}[Q_m]^{-1}[D]^{-1}[C]^{\dagger}[P]\dot{\boldsymbol{X}}\right) \tag{37}$$

Substituting $\hat{s}$ in Eq. (37) into charge vector $\boldsymbol{Q}$ in Eq. (33) constructs the following saturated charge product control law:

$$\boldsymbol{Q} = [Q_m]\hat{\boldsymbol{s}} = -[Q_m]\text{sign}\left(\frac{1}{k_c}[Q_m]^{-1}[D]^{-1}[C]^{\dagger}[P]\dot{\boldsymbol{X}}\right) \tag{38}$$

The resulting actual Lyapunov function rate should be investigated because after taking the sign function of $\tilde{\boldsymbol{s}}$, the actual Lyapunov function rate is different from the nominal one in Eq. (35). Substituting the actual charge product in Eq. (33) into Eq. (32), yields

$$\dot{V}_2 = k_c\dot{\boldsymbol{X}}^T[C][D][Q_m]\boldsymbol{s} = k_c\dot{\boldsymbol{X}}^T[C][D][Q_m]\text{sign}(\tilde{\boldsymbol{s}}) \tag{39}$$

Note that the sign function can be deemed as a rescaling of the magnitude of the vector, introduce a scale matrix $[E] = \text{diag}(a_1, a_2, a_3)$, where a_i is defined as

$$a_i = \begin{cases} \frac{1}{\|\tilde{s}_i\|}, & \text{if } \tilde{s}_i \neq 0 \\ 0, & \text{if } \tilde{s}_i = 0 \end{cases} \tag{40}$$

Thus $\boldsymbol{s}$ can be rewritten as

$$\boldsymbol{s} = [E]\tilde{\boldsymbol{s}} \tag{41}$$

Substituting Eq. (41) into Eq. (39), and using Eq. (36) yields

$$\dot{V}_2 = k_c\dot{\boldsymbol{X}}^T[C][D][Q_m][E]\tilde{\boldsymbol{s}} = -\dot{\boldsymbol{X}}^T\underbrace{[C][D][Q_m][E][Q_m]^{-1}[D]^{-1}[C]^{\dagger}[P]}_{[F]}\dot{\boldsymbol{X}} \tag{42}$$

Without loss of generality, set the positive definite matrix $[P]$ to be a diagonal matrix:

$$[P] = \begin{bmatrix} p_1 & 0 \\ 0 & p_2 \end{bmatrix} \tag{43}$$

Utilizing previous definitions of matrices $[C]$, $[D]$, $[Q_m]$, $[E]$, and $[P]$, the matrix $[F]$ is expanded as:

$$[F] = \frac{1}{3}\begin{bmatrix} p_1(2a_1 + a_3) & p_2(-a_1 + a_3) \\ p_1(-a_2 + a_3) & p_2(2a_2 + a_3) \end{bmatrix} \tag{44}$$

From the condition $p_i > 0$, it can be verified that the matrix $[F]$ is positive definite if $a_i > 0$, it is positive semidefinite if $a_i \geq 0$. By the definition of matrix $[E]$, $a_i \geq 0$, so $[F]$ is positive semidefinite. Thus the sign of the Lyapunov function rate is determined:

$$\dot{V}_2 = -\dot{\boldsymbol{X}}^T[F]\dot{\boldsymbol{X}} \leq 0 \tag{45}$$

Thus the saturated control law in Eq. (37) is globally stable. But it's not asymptotically stable because the matrix $[F]$ can be zero if the states $\boldsymbol{X}$ grow infinitely large.

3.3.2 Implementable Saturated Control

The saturated charge product control in Eq. (38) provides a globally stable control that stops the relative motion of the formation. But this formula doesn't ensure physical implementability of the charge products. Similar to the shape control design, an implementable sign vector $\boldsymbol{s} = [s_1, s_2, s_3]$ should satisfy

$$s_1 \cdot s_2 \cdot s_3 > 0 \tag{46}$$

Unlike the case in the shape control design, the saturated control should be dealing with more cautions because the sign function (or the matrix $[E]$) scales everything inside of the brackets. Note that the matrix $[E]$ is also varying with the vector inside the sign function. A similar approach that explores the null space of a certain matrix doesn't easily work out because of the rescaling of the matrix $[E]$, and the coupling of the matrix $[E]$ with the vector inside the sign function.

Note that in designing the stabilizing saturated control using Lyapunov stability theory, the stability property is achieved by setting the Lyapunov function rate to be negative semi-definite. This is ensured by the positive-definite property of the 2×2 matrix $[P]$. In most cases, this matrix is constant because usually it's unnecessary to change the value of the matrix $[P]$ and a constant $[P]$ matrix may result in a better convergence property of the system. Because the saturated control in Eq. (38) is globally stable but not asymptotically stable, changing the matrix $[P]$ won't sacrifice convergence property of the system. Since the matrix $[P]$ is only required to be positive-definite to guarantee the stability of the system, there exists a flexibility in choosing $[P]$.

Without lose of generality, set the matrix $[P]$ to be diagonal: $[P] = \text{diag}(p_1,\ p_2)$. For $[P]$ to be positive-definite, the parameters p_1 and p_2 must be positive. Let p_1 and p_2 be constants, to set up a variable matrix $[P]$, introduce a variable parameter τ. The matrix $[P]$ is then expressed as

$$[P] = \begin{bmatrix} p_1 & 0 \\ 0 & \tau p_2 \end{bmatrix} \tag{47}$$

here $\tau > 0$ should be positive to ensure $[P]$ to be positive-definite. Note that because matrices $[Q_m]$ and $[D]$ are all positive-definite diagonal, the sign vector in Eq. (37) can be simplified as

$$\boldsymbol{s} = -\text{sign}([C]^\dagger[P]\dot{\boldsymbol{X}}) \tag{48}$$

Substituting the values of matrices $[C]^\dagger$ and $[P]$ into Eq. (48), the vector $\boldsymbol{s}$ is expanded as

$$\boldsymbol{s} = -\text{sign}\left(\frac{1}{3}\begin{bmatrix} 2p_1\dot{x}_{12} - \tau p_2\dot{x}_{23} \\ -p_1\dot{x}_{12} + 2\tau p_2\dot{x}_{23} \\ p_1\dot{x}_{12} + \tau p_2\dot{x}_{23} \end{bmatrix}\right) \tag{49}$$

For the sign vector $\boldsymbol{s}$ to result in an implementable control, the vector inside the sign function should satisfy

$$(2p_1\dot{x}_{12} - \tau p_2\dot{x}_{23})(-p_1\dot{x}_{12} + 2\tau p_2\dot{x}_{23})(p_1\dot{x}_{12} + \tau p_2\dot{x}_{23}) < 0 \tag{50}$$

transform the inequality in Eq. (50) to be:

$$g(\tau) = (p_2\dot{x}_{23}\tau - 2p_1\dot{x}_{12})(2p_2\dot{x}_{23}\tau - p_1\dot{x}_{12})(p_2\dot{x}_{23}\tau + p_1\dot{x}_{12}) > 0 \tag{51}$$

Now it is clear that to find an implementable control by varying the matrix $[P]$ is to find a proper parameter $\tau > 0$ that satisfies the inequality $g(\tau) > 0$. First the existence of a solution should be verified. When $\dot{x}_{23} > 0$, the inequality in Eq. (51) can be transformed to be

$$h(\tau) = \Big(\tau - \underbrace{\frac{2p_1\dot{x}_{12}}{p_2\dot{x}_{23}}}_{a_1}\Big)\Big(\tau - \underbrace{\frac{p_1\dot{x}_{12}}{2p_2\dot{x}_{23}}}_{a_2}\Big)\Big(\tau + \underbrace{\frac{p_1\dot{x}_{12}}{p_2\dot{x}_{23}}}_{-a_3}\Big) > 0 \tag{52}$$

For the third order function $h(\tau)$, it goes to infinity as $\tau \to \infty$. So there always exists $\tau > 0$ to make $h(\tau) > 0$.

If $\dot{x}_{23} < 0$, the inequality in Eq. (52) changes to be

$$h(\tau) < 0 \tag{53}$$

Note that (a_1, a_2, a_3) are three roots to the equation $h(\tau) = 0$, and they share the simple relation $\text{sign}(a_1) = \text{sign}(a_2) = -\text{sign}(a_3)$. When $a_1, a_2 > 0$ and $a_3 < 0$, then any $\tau \in (a_2, a_1)$ satisfies $h(\tau) < 0$. If $a_1, a_2 < 0$ and $a_3 > 0$, in this case any $\tau \in (0, a_3)$ satisfies $h(\tau) < 0$.

Note that $\dot{x}_{12} = 0$ or $\dot{x}_{23} = 0$ are transient states, unless $\dot{\boldsymbol{X}} = 0$ which means the relative motion has been rested. So it can be concluded that there always exists $\tau > 0$ that results in an implementable control.

4 DOMAINS OF CONVERGENCE

So far a two-stage control strategy has been presented to control the 1-D Coulomb formation. At first a saturated charge control is used to stop the relative motion of the 3 spacecraft. After the relative motion converges to zero, the formation shape control will be activated to make the spacecraft to form a certain shape defined by provided distances.

As mentioned before, the saturated charge control in Eq. (38) is globally stable, but not asymptotically stable. Under some initial conditions, such as the three spacecraft are flying apart each others too fast, the relative motion cannot be rested at all. There exist certain areas of the initial distances and distance rates for the relative motion to be restable. This section is going to find out the domains of convergence of the initial conditions that result in stabilizable motions.

4.1 Converge Criteria For Symmetric Relative Motion

Symmetric relative motion is a very special case in 1-D Coulomb formation. The distances between any two adjacent spacecraft are always equal to each other and the adjacent distance rates are also equal. That is

$$\delta x_{12} = \delta x_{23}, \quad \delta\dot{x}_{12} = \delta\dot{x}_{23} \tag{54}$$

And corresponding to this situation, the masses and charge limits of each body should all be equal, $m_1 = m_2 = m_3 = m$, $q_{1\max} = q_{2\max} = q_{3\max} = q_{\max}$. In this case, the description of the motion can be greatly simplified. It is an easy start in studying general motion of the 1-D Coulomb formation.

For the 1-D Coulomb formation, the situation that may most likely result in an unrestable motion is that three spacecraft are departing from each other. That is $\delta\dot{x}_{12} > 0$ and $\delta\dot{x}_{23} > 0$. The following discussion deals with this "worst" case to find the critical initial conditions. The unrestable motion happens when the center spacecraft attracts two other spacecraft, but the distance rate vector $\dot{\boldsymbol{X}}$ still doesn't decrease to zero. In this case the charges of the 3 spacecraft are

$$q_1 = q_3 = q_{\max}, \quad q_2 = -q_{\max} \tag{55}$$

Reference 13 presents an analytical way to find the criteria for a potential collision between 2 charged craft to be avoidable. It assumes that the charge product is constant, thus the trajectory of the 2-body motion is a conic section. Utilizing the technic from gravitational 2-body problem (2BP), the criteria is found through calculating the periapsis radius which is the closest distance between the 2 spacecraft in the conic section trajectory.

Motivated by the analytical approach to solve the 2-body Coulomb forced motion, another concept of the traditional gravitational 2BP, total energy level, is introduced to study the 3-body 1-D Coulomb formation. Note that in the gravitational 2BP, the hyperbola is a non-retrievable trajectory type, and it corresponds to an energy level that is greater than zero. By assuming that the charges of the spacecraft are constant, the total energy (kinetic energy and potential energy) of the 3-body system is constant. The unrestable motion corresponds to a positive energy level, and the stabilizable motion has a total energy that is negative.

The general relative kinetic energy T_{rel} is given by Eq. (16). Using the symmetric conditions provided above, T_{rel} is simplified to be

$$T_{rel} = \frac{m^2}{2M}\delta\dot{x}_{12}^2 + \frac{m^2}{2M}(\delta\dot{x}_{12} + \delta\dot{x}_{23})^2 + \frac{m^2}{2M}\delta\dot{x}_{23}^2 = \frac{M}{3}\delta\dot{x}_{12}^2 \tag{56}$$

where $M = 3m$ is the total formation mass. The electrostatic potential energy of the formation is

$$V_e = k_c\frac{Q_{12}}{\delta x_{12}} + k_c\frac{Q_{23}}{\delta x_{23}} + k_c\frac{Q_{13}}{\delta x_{12} + \delta x_{23}} \tag{57}$$

Utilizing the symmetric motion condition in Eq. (54) and Eq. (55), V_e is simplified as

$$V_e = k_c\left(-\frac{q_{\max}^2}{\delta x_{12}} - \frac{q_{\max}^2}{\delta x_{12}} + \frac{q_{\max}^2}{2\delta x_{12}}\right) = -\frac{3k_c q_{\max}^2}{2\delta x_{12}} \tag{58}$$

Thus the total energy is the sum of the kinetic energy and potential energy:

$$E_e = T_{\text{rel}} + V_e = \frac{M}{3}\delta\dot{x}_{12}^2 - \frac{3k_c q_{\max}^2}{2\delta x_{12}} \tag{59}$$

which has a very simple form due to the symmetric relative motion assumption. Because the charges of the spacecraft are constants in this saturated control discussion, the total energy is also constant. For a stabilizable motion, the total energy E_e should be negative, that is

$$E_e = \frac{M}{3}\delta\dot{x}_{12}^2 - \frac{3k_c q_{\max}^2}{2\delta x_{12}} < 0 \tag{60}$$

If $E_e < 0$, then it is impossible for $\delta x_{12} \to \infty$. However, if $E_e > 0$, then $\delta \dot{x}_{12}$ will approach a positive value as $\delta x_{12} \to \infty$. Transforming Eq. (60) such that only δx_{12} and $\delta \dot{x}_{12}$ remain on the left hand side yields the condition

$$\delta \dot{x}_{12}^2 \delta x_{12} < \frac{9 k_c q_{\text{max}}^2}{2M} = \frac{3 k_c q_{\text{max}}^2}{2m} \tag{61}$$

Eq. (61) provides an analytical criteria of the initial states δx_{12} and $\delta \dot{x}_{12}$ to result in a stabilizable symmetric motion. From the criteria, it can be seen that when the charges and masses of the three spacecraft are set, both the distance and distance rate should be within a certain range to ensure the symmetric relative motion can be stopped. Note that as expected a bigger charge level will result in a larger area of stabilizable motion. This criteria is valid only for the symmetric relative motion of the 1-D Coulomb formation. The following discussion will investigate the converge area of general motion of the 1-D Coulomb formation.

4.2 Converge Area For General Cases

The previous subsection derives the convergence criteria for the symmetric relative motion by investigating the total energy of the system. Because the sign of the spacecraft charges are varying even while the magnitudes are maintained, the energy of the system is not constant. It's very difficult to apply a similar approach as in the symmetric motion to analyze the general converge area of the saturated control.

Instead, this sections presents a numerical study of the general convergence areas of the initial conditions. Usually the convergence area is illustrated by marking each set of initial conditions for which the distance rates converge to zero in the numerical simulation. Without the assumption of symmetric motion, the initial conditions of the motion contain four independant variables: $[\delta x_{12}, \delta x_{23}, \delta \dot{x}_{12}, \delta \dot{x}_{23}]$. Thus the convergence area should be configured as a four dimensional region. To illustrate the convergences areas in 2-dimensional plots, the distances and distance rates are illustrated separately. A certain set of initial $[\delta \dot{x}_{12}, \delta \dot{x}_{23}]$ is prescribed, the convergence area of initial variables $[\delta x_{12}, \delta x_{23}]$ is illustrated in a 2-D phase plane. And the convergence area of the variables $[\delta \dot{x}_{12}, \delta \dot{x}_{23}]$ is demonstrated in the similar way in the $\delta \dot{x}_{12} - \delta \dot{x}_{23}$ plane.

Taking the 1-D non-conducting hover track vehicles as an example, let the masses be $m_1 = m_2 = m_3 = 10$kg, and the charge limits be $q_{1\text{max}} = q_{2\text{max}} = q_{3\text{max}} = q_{\text{max}} = 5 \times 10^{-5}$C. Let the feedback control gain parameters be $p_1 = p_2 = 1\text{kg}/(\text{C}^2 \cdot \text{s})$. Figure 4 shows the converge areas of the distances δx_{12}, δx_{23} under different initial distance rates. Figure 4(a) shows the case when the initial distance rates $[\delta \dot{x}_{12}, \delta \dot{x}_{23}] = [0.1, 0.1]$m/s. These results illustrate how close the craft must be placed if their initial velocities are not perfectly zero, but bounded by 0.1 m/s. The shaded region represents initial positions which result in converged states, the initial position coordinates outside of this area will not lead $[\delta \dot{x}_{12}, \delta \dot{x}_{23}]$ to converge to zero. The convergence area is not quite symmetric in δx_{12} and δx_{23} direction. This is because the implementation strategy which varies the matrix $[P]$ doesn't result in symmetric solutions while switching the values of the individual distances δx_{12} and δx_{23}. Figure 4(b) shows the convergence area of the $\delta x_{12} - \delta x_{23}$ plane when the initial distance rates are set to be $[\delta \dot{x}_{12}, \delta \dot{x}_{23}] = [0.1, 0.2]$m/s. The convergence area shrinks along both δx_{12} and δx_{23} axes, but more greatly in the δx_{23} direction. Because the departure speed of $\delta \dot{x}_{23}$ is larger than $\delta \dot{x}_{12}$, it takes more time for $\delta \dot{x}_{23}$ to converge to zero than that of $\delta \dot{x}_{12}$.

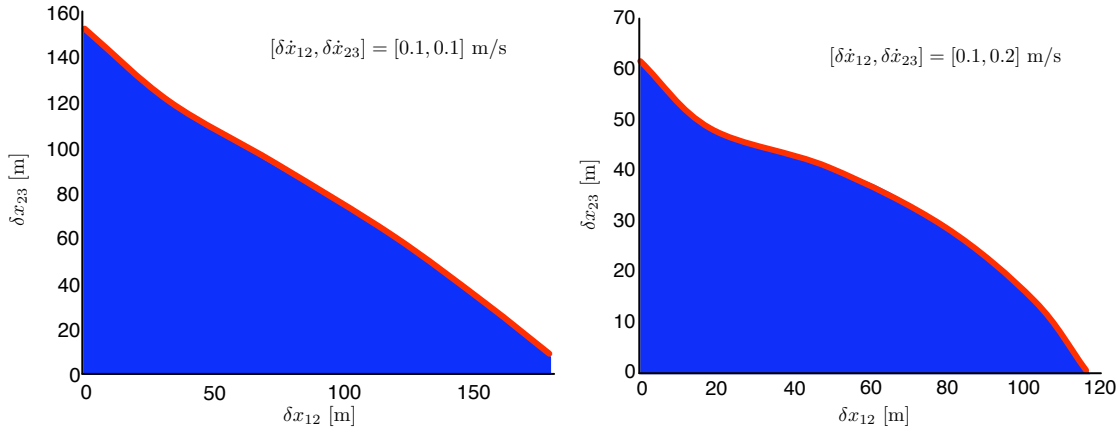

(a) $(\delta\dot{x}_{12}, \delta\dot{x}_{23}) = (0.1, 0.1)$m/s. (b) $(\delta\dot{x}_{12}, \delta\dot{x}_{23}) = (0.1, 0.2)$m/s.

Figure 4 Convergence area of $(\delta x_{12}, \delta x_{23})$.

Figure 5 illustrates two converge areas of the distance rates in the $\delta\dot{x}_{12} - \delta\dot{x}_{23}$ plane. This setup assumes the craft are place a particular distance apart, and then investigates how large the initial separation rates can be and still achieve convergence. It can be seen that the convergence area reduces in the direction where the distance increases. The plots show $\delta\dot{x}_{ij}$ ranging within $[-0.2, 0.8]$m/s. The negative distance rate means the two spacecraft are approaching each other. If the magnitude of the negative distance rate is too big, then the spacecraft are getting close too fast, this may result in a collision of the spacecraft which is not discussed in this paper. Rather, Reference 13 develops the analytical criteria for two spacecraft which are approaching each other to be able to avoid the collision.

5 NUMERICAL SIMULATION

A two-stage control strategy is developed in this paper to control the shape of the 1-D constrained Coulomb structure. At first the saturated control is used to rest the relative motion of the spacecraft. After the relative motion has been stabilized, the formation shape controller is employed to make the formation construct a certain shape which is defined by the states $[\delta x_{12}^*, \delta x_{23}^*]$. This section presents some numerical simulation results to show the performance of the control strategy.

The simulation parameters are set to reflect those of a small hover track setup. The masses of the three spacecraft are $m_1 = m_2 = m_3 = 10$kg, the desired shape is given as $[\delta x_{12}^*, \delta x_{23}^*] = [4, 4]$m. The separation distances between craft are within 5 meters. Without loss of generality, let the magnitudes of the charges of the spacecraft share a unique limit $q_{\max} = 5 \times 10^{-5}$C. Choose the initial inertial positions and velocities to be:

$$[x_1, x_2, x_3] = [-3, 0, 2] \text{ m} \tag{62}$$

$$[\dot{x}_1, \dot{x}_2, \dot{x}_3] = [-0.04, 0, 0.04] \text{ m/s} \tag{63}$$

Figure 6 shows the first stage of the control which uses the saturated control to arrest any relative motion. The two stages of simulation results are illustrated separately because the saturated control achieves its control goal over a much shorter time span than the unsaturated shape control. The states

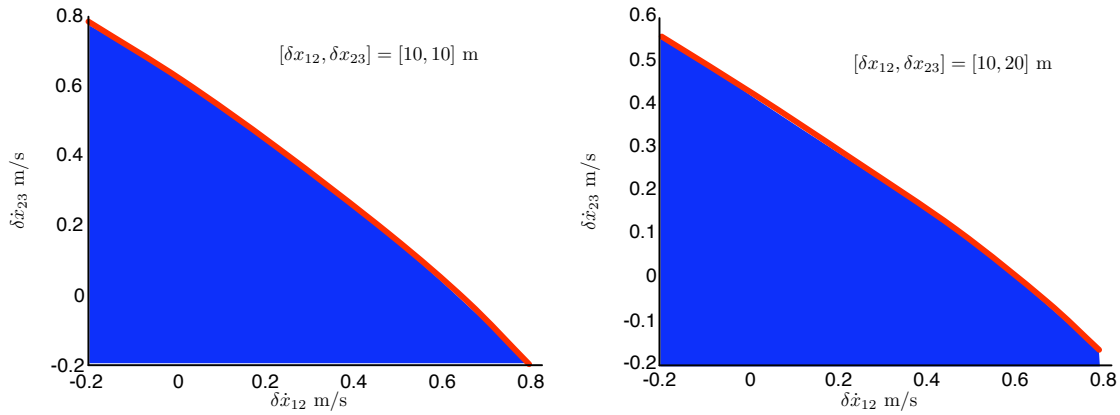

(a) $(\delta x_{12}, \delta x_{23}) = (10, 10)$m. (b) $(\delta x_{12}, \delta x_{23}) = (10, 20)$m.

Figure 5 Convergence area of $(\delta\dot{x}_{12}, \delta\dot{x}_{23})$.

of the two stage are continuous, here the state historiy illustrations are split at the time when the relation motion is rested. The control feedback parameters of the saturated regulator are $p_1 = p_2 = 1\text{kg}/(\text{C}^2\cdot\text{s})$. The relative distance rates converge to zero in a very short time, and the control charges are always saturated until the distance rates converge. The stability of the control is guaranteed, and if the initial conditions are within the convergence area presented in the last section, the relative motion can be arrested.

Figure 7 illustrates the simulation results of the second stage, the unsaturated formation shape control. The parameters of this control are

$$[K] = \begin{bmatrix} 3.6 & 0 \\ 0 & 1.8 \end{bmatrix} \text{kg}\cdot\text{m/s}^2, \qquad [P] = \begin{bmatrix} 14.4 & 0 \\ 0 & 7.2 \end{bmatrix} \text{kg}\cdot\text{m/s} \tag{64}$$

Figure 7(a) and (b) show the process of the Coulomb structure to converge to the desired shape. Figure 7(c) and (d) are the charge histories under different conditions. The chattering issue of the charges is nontrivial in the control process. As mentioned before in the formation shape control section, the chattering effect is partly due to the switching between two possible values of the variable τ. The parameter $\alpha \leq 1$ has been introduced to buffer the switching. With $\alpha = 1$, no buffer is acting on the system. When $0 < \alpha < 1$, the buffer is taking effect. Comparing Figure 7(c) and (d), it can be seen that when $\alpha = 0.7$, the chattering effect is reduced to some extent. Though the buffer can not totally eliminate the chattering, the benefit is that this approach will not influence the dynamics of the system. This is because any value of the variable τ results in a vector that is within the null space of the input matrix of the control.

6 CONCLUSION

A two-stage stable charge feedback control strategy is developed to shape the configuration of the 1-D restricted Coulomb structure. The first stage is a saturated control strategy intended to arrest the relative motion of the formation. The control is designed using Lyapunov's direct method. It's globally stable, but not globally asymptotically stable. Only for a finite neighborhood of initial states will the separation distance rates converge to zero. For the symmetric motion case, the

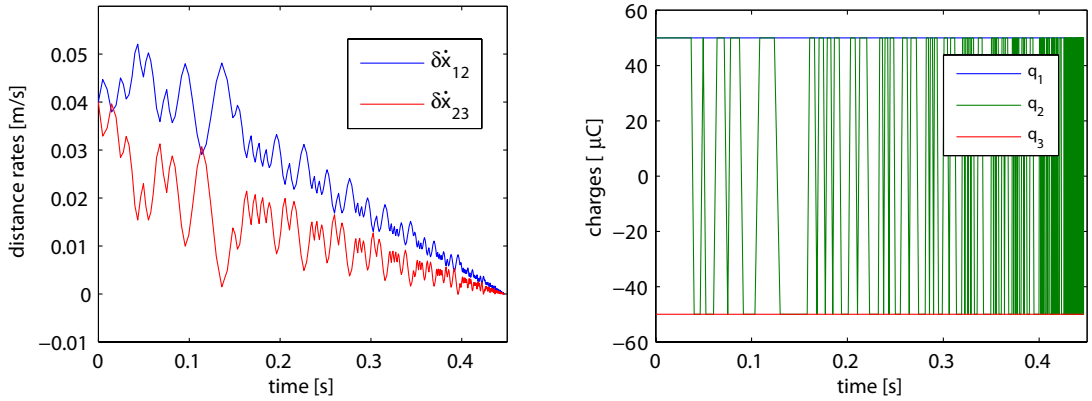

(a) Separation distance rates.

(b) Control charges' histories.

Figure 6 Stage I: relative motion regulator.

analytical criteria for a stabilizable motion is obtained by investigating the total energy level of the system. Numerical results are presented to illustrate the convergence area of the initial states of stabilizable motions for general cases. The implementability issue of the saturated control is solved through varying the value of the positive definite feedback gain matrix which is used in designing the Lyapunov function rate. The second stage is a non-saturated formation shape control. It's used to control the shape of the Coulomb structure to a certain desired configuration. The control is also designed using Lyapunov's direct method. A minimum charge search routine in the null space of the plant matrix is used to solve the control charge implementability problem. The search routine not only makes the charge control law physically implementable, but also results in minimum control charges at every instance. Numerical simulations verify the effectiveness of the control strategy.

REFERENCES

[1] L. B. King, G. G. Parker, and S. D. e. al., "Spacecraft Formation Flying using Inter-Vehicle Coulomb Forces," *Tech. rep., NASA/NIAC*, January 2002.

[2] E. M. C. Kong and D. W. K. e. al., "Electromagnetic Formation Flight for Multisatellite Arrays," *Journal of Spacecraft and Rockets*, Vol. 41, July-August 2004.

[3] L. B. King, G. G. Parker, S. Deshmukh, and J.-H. Chong, "A Study of Inter-Spacecraft Coulomb Forces and Implications for Formation Flying," *38th AIAA/ASME/SAE/ASEE Joint Propulsion Conference Exhibit, Indianapolis, Indiana*, July 2002.

[4] H. Joe, H. Schaub, and G. G. Parker, "Formation Dynamics of Coulomb Satellites," *6th International Conference on Dynamics and Control of Systems and Structures in Space*, July 18-22 2004.

[5] G. G. Parker, C. E. Passerello, and H. Schaub, "Static Formation Control Using Interspacecraft Coulomb Forces," *2nd International Symposium on Formation Flying Missions and Technologies*, Sept. 14-16 2004.

[6] H. Schaub and M. Kim, "Differential Orbit Element Constraints for Coulomb Satellite Formations," *Astrodynamics Specialist Conference*, Aug. 16–19 2004.

[7] A. Natarajan and H. Schaub, "Linear Dynamics and Stability Analysis of a Coulomb Tether Formation," *AIAA Journal of Guidance, Control, and Dynamics*, Vol. 29, July–Aug. 2006, pp. 831–839.

[8] A. Natarajan, H. Schaub, and G. G. Parker, "Reconfiguration of a Nadir-Pointing 2-Craft Coulomb Tether," *Journal of British Interplanetary Society*, Vol. 60, June 2007, pp. 209–218.

[9] A. Natarajan and H. Schaub, "Hybrid Conrol of Orbit Normal and Along-Track 2-Craft Coulomb Tethers," *AAS Space Flight Mechanics Meeting*, Sedona, AZ, Jan. 28–Feb. 1 2007. Paper AAS 07–193.

[10] S. Wang and H. Schaub, "One-Dimensional 3-Craft Coulomb Structure Control," *7th International Conference on Dynamics and Control of Systems and Structure in Space*, Greenwich, London, England, June 14-16 2006.

[11] J. Berryman and H. Schaub, "Analytical Charge Analysis for 2- and 3-Craft Coulomb Formations," *AAS/AIAA Astrodynamics Specialists Conference*, Lake Tahoe, CA, Aug. 7–11, 2005 2005. Paper No. 05-278.

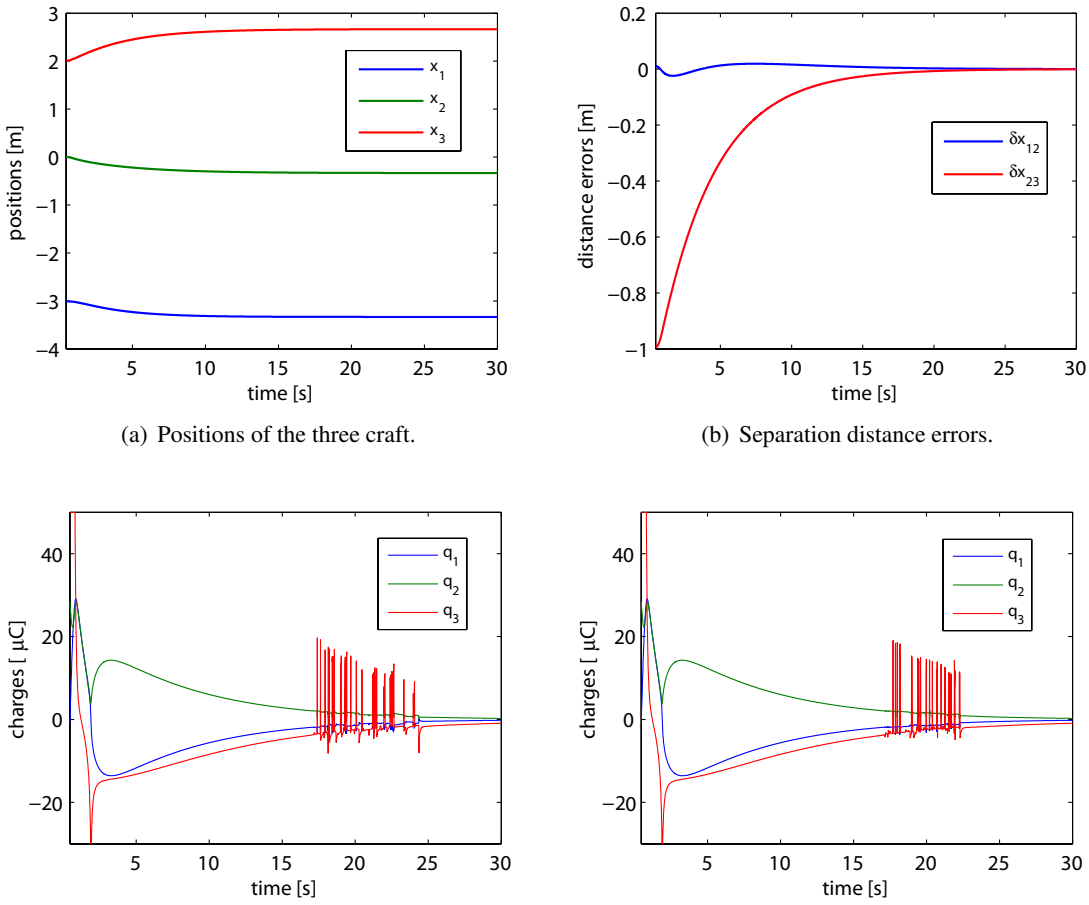

(a) Positions of the three craft.

(b) Separation distance errors.

(c) Control charges' histories when $\alpha = 1$.

(d) Control charges' histories when $\alpha = 0.7$.

Figure 7 Stage II: formation shape control.

[12] R. D. Robinett, G. G. Parker, H. Schaub, and J. L. Junkins, "Lyapunov Optimal Saturated Control for Nonlinear Systems," *AIAA Journal of Guidance, Control, and Dynamics*, Vol. 20, Nov.–Dec. 1997, pp. 1083–1088.

[13] S. Wang and H. Schaub, "Spacecraft Collision Avoidance Using Coulomb Forces With Separation Distance Feedback," *17th AAS/AIAA Space Flight Mechanics Meeting*, Sedona, Arizona, AAS/AIAA, January28-February 1 2007.